DALTON
FULL PAPER

Magnetostructural behaviour of the complex $[MnL(H_2O)_2]Cl_2\cdot 4H_2O$ at variable temperature studied by electron spin resonance (L = 2,13-dimethyl-3,6,9,12,18-pentaazabicyclo[12.3.1]octadeca-1(18),2,12,14,16-pentaene)

Omar Jiménez-Sandoval,[a] Daniel Ramírez-Rosales,[b] María del Jesús Rosales-Hoz,[c] Martha Elena Sosa-Torres*,†,[a] and Rafael Zamorano-Ulloa[b]

[a] *División de Estudios de Posgrado, Facultad de Química, Universidad Nacional Autónoma de México, Ciudad Universitaria, México, D. F. 04510, México*
[b] *Depto. de Física, Escuela Superior de Fisica y Matemáticas del IPN, Edif. 9, U. P. Zacatenco, Col. San Pedro Zacatenco, México, D. F. 07738, México*
[c] *Depto. de Química, Centro de Investigación y Estudios Avanzados del IPN, Apartado Postal 14-740, México, D. F. 07000, México*

The molecular and crystal structure of the complex $[MnL(H_2O)_2]Cl_2\cdot 4H_2O$ **1** (L = 2,13-dimethyl-3,6,9,12,18-pentaazabicyclo[12.3.1]octadeca-1(18),2,12,14,16-pentaene) have been determined, the solid state and solution electronic spectra recorded and the thermogravimetric analysis as well as an ESR analysis at different temperatures performed. The structure shows that the cation displays a distorted pentagonal-bipyrimidal co-ordinated geometry, with the macrocycle in the pentagonal plane and two water molecules in the axial positions. From the UV/VIS spectra it can be seen that the electronic structure of **1** is very sensitive to surroundings. The 300 K ESR spectrum of **1** consists of five fine-structure lines centred at $g = 2.111$, showing anisotropy. A sequence of spectra neatly shows that the compound has a clear magnetic dependence on temperature. Spectral analysis and theoretical calculations give the best 300 K zero-field splitting parameters as $D = 0.07$ cm^{-1}, $E = 0.008$ cm^{-1}, $\lambda = E/D = 0.1142$. The 77 K zero-field splitting parameters increase to $D = 0.074$ cm^{-1} and $E = 0.012$ cm^{-1}, thus indicating an increasing rhombic distortion as the temperature decreases. The Q-band spectra at 300 and at 77 K are isotropic, and the zero-field effects are very small. The theoretical Q-band spectra were calculated on the basis of the X-band parameters. The temperature variation of the crystal-field parameters is interpreted as a smooth magnetostructural temperature dependence of the compound.

The booming development that the chemistry of macrocyclic ligand complexes has experienced in the last few decades is well founded on the interesting structural, thermodynamic, kinetic and magnetic properties that such compounds display. Another key factor in their development and study is their possible usage as models for important biological systems that involve metal ions co-ordinated to macrocycles.[1] Moreover, the co-ordination chemistry of manganese has been important for the better understanding of the O_2 evolution mechanism in the photosynthetic process.[2]

Additional interest bears on totally or partly unsaturated macrocyclic compounds, the lack of flexibility of which results in a restriction of their possible co-ordination modes to metal ions, thus forcing the metal in some cases to accommodate uncommon geometries[3] and promoting an enhancement of the stabilising macrocyclic effect.[4]

The 15-membered, pentadentate macrocycle 2,13-dimethyl-3,6,9,12,18-pentaazabicyclo[12.3.1]octadeca-1(18),2,12,14,16-pentaene, L, has been found to adopt a planar conformation, imposing a pentagonal-based geometry on metal ions of different electronic configurations,[5] leading to the stabilisation of seven-co-ordinate species.[6]

Here we report the synthesis, molecular and crystal structure, solid-state and solution electronic spectra, thermogravimetric analysis, and variable-temperature ESR study at X and Q band of the compound $[MnL(H_2O)_2]Cl_2\cdot 4H_2O$ **1**.

The structure of the $[MnL(H_2O)_2]^{2+}$ cation, as its PF_6 salt, has been reported,[7] however no details were given nor was the precision of the X-ray determination evaluated. A more recent report,[8] on the $[MnL(H_2O)_2]Cl[ClO_4]$ complex, is mainly concerned with other features and provides little discussion on the crystal structure of the manganese cation. On the other hand, the ESR spectrum of $[MnL]Cl_2\cdot 6H_2O$ was the subject of an earlier report,[9] however only room-temperature results were provided.

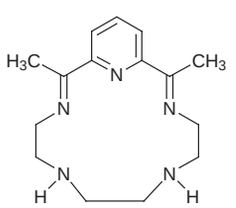

L

Experimental

Synthesis

The compound was obtained by reaction of stoichiometric amounts of 2,6-diacetylpyridine (0.75 g, 4.6 mmol), 3,6-diazaoctane-1,8-diamine (0.675 g, 4.6 mmol), and $MnCl_2\cdot 4H_2O$ (0.9 g, 4.5 mmol) by using a slight modification of the synthesis reported by Humanes.[10] The amine was added dropwise to a hot solution of the metal salt and diacetylpyridine in water (12.5 cm^3). After a 3 h reflux the hot reaction mixture was filtered and the dark brown tarry residue discarded. The deep orange solution was then allowed to cool, rendering deep orange crystals of the compound, suitable for X-ray diffractometry [71% yield, m.p. = 267 °C (decomp.)] (Found: C, 35.46; H, 7.00; N, 13.62. $C_{15}H_{35}Cl_2MnN_5O_6$ requires C, 35.51; H,

† E-mail: mest@servidor.unam.mx

6.95; N, 13.80%). IR (KBr)[11]: 3358s [ν(OH)], 3270s [ν(NH)], 2906m [$\nu_{asym}(CH_2)$], 2852s [$\nu_{sym}(CH_3)$], 1648s [ν(C=N)], 1584m [ν(C=C)], 1458m [$\delta_{asym}(CH_3)$], 1376m [$\delta_{sym}(CH_3)$] and 546mw (OH, co-ordinated water).

Crystallography

Unit cell dimensions with estimated standard deviations were obtained from least-squares refinements of the setting angles of 25 carefully centred reflections. Two standard reflections monitored periodically showed no change during the data collection. A summary of important crystallographic data is presented in Table 1. Corrections were made for Lorentz-polarisation effects. The atomic scattering factors were taken from refs. 12 and 13.

The structure was solved by direct methods by using the CRYSTALS package[14] and refined by full-matrix least-squares cycles. Anisotropic thermal parameters were introduced for all non-hydrogen atoms. Hydrogen atoms were found on difference electron-density maps and refined isotropically.

CCDC reference number 186/928.

ESR measurements

Since the single crystals used for the X-ray studies were not of suitable size for ESR measurements, these studies were carried out on polycrystalline samples at X and Q band on a JEOL JES-RES3X spectrometer, operating at 100 KHz and equipped with a laboratory-made X-band low-temperature accessory for the 77 K experiments. The manganese(II) complex shows a broad unresolved singlet centred at around $g = 2.0$. In order to obtain resolved spectra, the compound was magnetically diluted into a diamagnetic rhodium matrix {*cis*[$RhCl_2$(cyclam)]Cl} to a final concentration of 9.52% (w/w). The ESR X-band spectra were recorded at variable temperature, ranging from 300 down to 77 K. The *g* value was calculated from the accurate measurements of magnetic field and frequency parameters. The Q-band spectra were recorded using a JEOL ES-SQ4 microwave cavity and a ES-UTQ3 Q-band variable-temperature system. Additionally, dilutions of **1** in dimethyl sulfoxide were prepared and studied at 77 K, at X-band frequency.

Theoretical spectra were calculated by means of a set of programs, run in MATLAB, especially developed for this purpose by our group.[15] The method includes matrix diagonalisation and numerical exact eigenvalues, eigenfunction solutions, transition probabilities and transition fields, along the lines of the calculations made by Dowsing and Gibson,[16] Griscom and Griscom,[17] and more recently Pilbrow[18] and Mabbs and Collison.[19]

Other measurements

The elemental analyses (C, H and N) were carried out on a Perkin-Elmer 240B microanalyser at University College London. Infrared spectra of KBr pellets of the complex were recorded on a Perkin-Elmer 599-B spectrophotometer, in the range 4000–200 cm^{-1}, electronic spectra of the solid sample on a Cary 5E UV/VIS-NIR spectrophotometer, aqueous solutions on a Hewlett-Packard 8452A diode-array spectrophotometer. Thermogravimetric analysis was performed on a 951 Du Pont Thermogravimetric analyser. Magnetic susceptibility was measured on a Faraday balance at room temperature. Diamagnetic corrections were made by using Pascal's constants. The set-up was calibrated with $Hg[Co(SCN)_4]$ as standard.

Results and Discussion

The compound was formulated as $[MnL]Cl_2\cdot 6H_2O$ when first synthesized by Alexander *et al.*,[20] considering the two chlorine atoms co-ordinated to the manganese(II) ion in CH_3NO_2 solutions, but dissociated in water. A second formulation, containing the $[MnL(H_2O)_2]^{2+}$ cation, was proposed by Drew *et al.*[21] on the basis of spectroscopic and conductance studies. This cation was later found in the crystal structure of the related compound $[MnL(H_2O)_2][PF_6]_2$, however, as previously pointed out, only very scarce structural data were provided.[7]

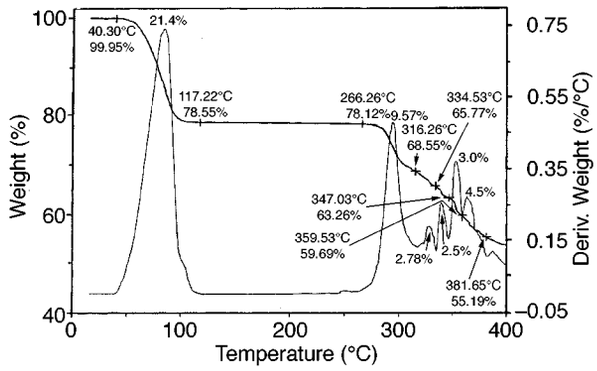

Fig. 1 Thermogram of $[MnL(H_2O)_2]Cl_2\cdot 4H_2O$, run under N_2 and at 5 °C min^{-1}

The thermogravimetric analysis for the previously reported $[MnL(H_2O)_2][PF_6]_2$ compound[7] does not show the same pattern as that of our complex, Fig. 1. The latter is very clear and reveals a single weight loss (21.4%, 40–117 °C) before decomposition, corresponding to all the six H_2O molecules (21.3%), without differentiation between co-ordination and crystallisation water (even though the sample was heated at 5 °C min^{-1}). In contrast, the two co-ordinated H_2O molecules in the PF_6 salt[7] are lost at lower temperatures (80–100 °C).

Compound **1** has a magnetic moment of 6.0 μ_B ($\mu_B \approx 9.27 \times 10^{-24}$ J T^{-1}) and hence is a high-spin system. It is light yellow in aqueous solution, but gives strong absorptions at 294, 256 and 230 nm in the UV region. These bands are probably associated with charge-transfer transitions of the pyridine-imine site, as pointed out previously.[21] There is also a weak band ($\varepsilon = 140$ dm^3 mol^{-1} cm^{-1}) in the visible region, at 400 nm. The ground term for a d^5 configuration is the orbital singlet ^6S, which cannot be split by a crystal field of any symmetry. The absence of any other spin sextet terms requires that all transitions in high-spin d^5 complexes are spin- as well as Laporte-forbidden. However, if the orbital angular momentum is not completely quenched, the spin–orbit interaction mixes the ground state with the first excited states and then otherwise forbidden transitions have small probabilities. Therefore, if present, they will generally be very weak,[22] in complete agreement with our experimental observations. Hence, **1** is proposed to have as the ground term the orbital singlet ^6S mixed with excited states. The ESR spectroscopic *g* value is then expected to show some anisotropy and be centred around 2.0, since it is a spin $S = \frac{5}{2}$ weak crystal-field system. The visible absorption obtained in the solid state at room temperature appears at 445 nm, shifted from that in aqueous solution. This shift of 45 nm indicates that the form of **1** in aqueous solution is substantially different from that in the solid state, showing that the electronic structure is very sensitive to the surroundings.

Crystal structure

The system comprises the $[MnL(H_2O)_2]^{2+}$ cation (Fig. 2), two chloride counter ions and four crystallisation water molecules. Important lengths and angles are collected in Table 2. The cationic unit shows a slightly distorted pentagonal-bipyrimidal co-ordination geometry with the macrocycle in the pentagonal plane and two water molecules in the axial positions. The angle between the planes formed by the five nitrogen and the manganese atom and the plane including the metal and the two oxygen atoms is 89.8°.

The pentagonal plane is slightly distorted with N(1) being

Table 1 Summary of crystallographic data of $[MnL(H_2O)_2]Cl_2{\cdot}4H_2O$

Formula	$C_{15}H_{35}Cl_2MnN_5O_6$
M	507.31
Crystal symmetry	Monoclinic
Space group	$P2_1/n$
Crystal size/mm	0.5 × 0.5 × 0.3
a/Å	11.130(1)
b/Å	8.613(1)
c/Å	24.883(5)
β/°	95.22(5)
U/Å^3	2373.3(5)
Z	4
$F(000)$	1068
Diffractometer	Enraf-Nonius CAD4
Radiation (λ/Å)	Mo-Kα (0.710 69)
μ/cm^{-1}	7.97
D_c/g cm^{-3}	1.42
Scan type	ω–2θ
Scan range/°	0.8 + 0.345 tan θ
θ Limits/°	1–25
T	Room temperature
Octants collected	0–13, −10 to 0, −28 to 28
No. data collected	4229
No. unique data	3891
No. unique data used	3500 $[(F_o)^2 > 3\sigma(F_o)^2]$
R_{int}	1.78
Absorption correction	DIFABS[12] (minimum = 0.84, maximum = 1.13)
$R = \Sigma(\|\|F_o\| - \|F_c\|\|)/\Sigma\|F_o\|$	0.028
$R' = [\Sigma w(\|F_o\| - \|F_c\|)^2/\Sigma w F_o^2]^{\frac{1}{2}}$	0.031
Goodness of fit s	0.97
No. variables	411
$\Delta\rho_{min}$, $\Delta\rho_{max}$/e Å^{-3}	−0.97, 0.97

Table 2 Selected bond lengths (Å), angles (°) and torsion angles (°) for $[MnL(H_2O)_2]Cl_2{\cdot}4H_2O$

Mn–O(1)	2.259(2)	Mn–O(2)	2.249(2)
Mn–N(1)	2.298(2)	Mn–N(4)	2.286(2)
Mn–N(7)	2.254(2)	Mn–N(10)	2.289(2)
Mn–N(13)	2.316(2)		
O(1)–Mn–O(2)	174.99(9)	O(1)–Mn–N(1)	88.00(8)
O(2)–Mn–N(1)	87.32(8)	O(1)–Mn–N(4)	84.63(8)
O(2)–Mn–N(4)	92.33(8)	N(1)–Mn–N(4)	73.44(8)
O(1)–Mn–N(7)	89.01(8)	O(2)–Mn–N(7)	93.68(8)
N(1)–Mn–N(7)	143.21(8)	N(4)–Mn–N(7)	69.77(7)
O(1)–Mn–N(10)	96.34(8)	O(2)–Mn–N(10)	88.55(8)
N(1)–Mn–N(10)	147.14(8)	N(4)–Mn–N(10)	139.32(8)
N(7)–Mn–N(10)	69.59(7)	O(1)–Mn–N(13)	84.09(9)
O(2)–Mn–N(13)	96.48(9)	N(1)–Mn–N(13)	75.91(9)
N(4)–Mn–N(13)	147.62(8)	N(7)–Mn–N(13)	140.09(8)
N(10)–Mn–N(13)	72.20(8)	Mn–N(1)–C(2)	107.8(2)
Mn–N(1)–C(15)	109.7(2)	C(2)–N(1)–C(15)	114.3(2)
Mn–N(4)–C(3)	116.0(2)	Mn–N(4)–C(5)	120.9(2)
C(3)–N(4)–C(5)	123.1(2)	Mn–N(7)–C(6)	119.2(2)
Mn–N(7)–C(8)	119.7(2)	C(6)–N(7)–C(8)	121.0(2)
Mn–N(10)–C(9)	120.0(2)	Mn–N(10)–C(11)	117.1(2)
C(9)–N(10)–C(11)	121.6(2)	Mn–N(13)–C(12)	108.4(2)
Mn–N(13)–C(14)	108.7(2)	C(12)–N(13)–C(14)	115.0(3)
Mn–N(1)–C(2)–C(3)	−52.72	Mn–N(13)–C(12)–C(11)	−19.70
Mn–N(1)–C(15)–C(14)	−42.89	Mn–N(13)–C(14)–C(15)	−43.12
Mn–N(4)–C(3)–C(2)	22.60	N(1)–C(2)–C(3)–N(4)	−49.91
Mn–N(4)–C(5)–C(6)	2.11	N(4)–C(5)–C(6)–N(7)	−3.70
Mn–N(7)–C(6)–C(5)	3.63	N(7)–C(8)–C(9)–N(10)	9.35
Mn–N(7)–C(8)–C(9)	−3.28	N(10)–C(11)–C(12)–N(13)	−47.94
Mn–N(10)–C(9)–C(8)	−11.15	N(13)–C(14)–C(15)–N(1)	59.99
Mn–N(10)–C(11)–C(12)	−19.70		

0.19 Å above it, a larger deviation from planarity than that observed in a similar manganese complex derived from a 15-membered N_3O_2 macrocycle.[23] By contrast, another manganese complex derived from a larger 17-membered macrocycle[21] shows larger deviations from planarity.

The angles within the co-ordination sphere are close to expected values. All O (co-ordinated water)–Mn–N (macrocycle) angles are within 6° of 90° and the O(1)–Mn–O(2) angle

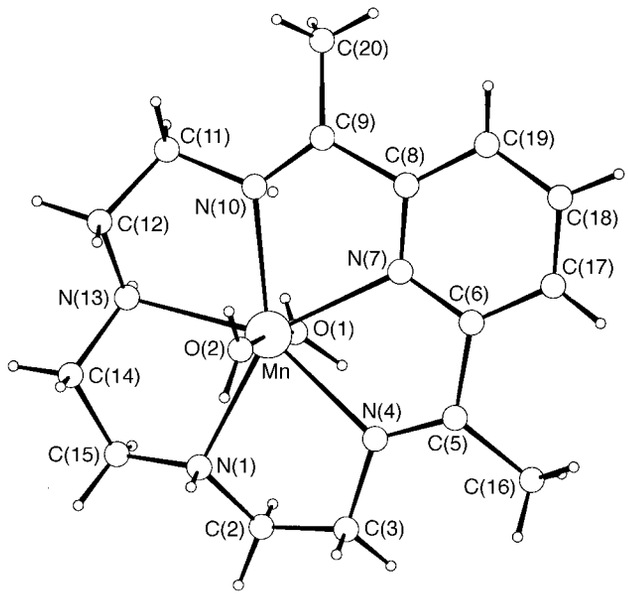

Fig. 2 Molecular structure of $[MnL(H_2O)_2]Cl_2{\cdot}4H_2O$

is 174.99(9)°. The pyridine ring forms an angle of 1.0° with the MnN_5 plane, smaller than in the N_3O_2 complex, where the value of 5.7° was believed to be due to a greater difficulty in accommodating the manganese ion in the macrocycle cavity.[23]

The conformation of the macrocycle can be appreciated from the torsion angles shown in Table 2. The two five-membered rings, which include the two imine bonds [Mn–N(4)–C(5)–C(6)–N(7) and Mn–N(7)–C(8)–N(10)], are nearly planar with maximum deviations of 0.06 Å. The remaining five-membered rings, as expected, are not planar and show atoms at about 0.3 Å above and below the square planes. There are some significant differences in the Mn–N distances with values ranging from 2.254(2) to 2.316(2) Å, the shortest bond corresponding to Mn–N(7), the only pyridine nitrogen atom. This bond was also the shortest in the MnN_3O_2 compound referred to above[23] and in the iron complex derived from the same quinquedentate ligand,[24] presumably due to the different hybridisation of the nitrogen atom. These Mn–N distances in **1** seem to be, even considering experimental error, longer than in the mentioned manganese and iron complexes of similar macrocycle size.

The manganese–oxygen distance [2.249(2) and 2.259(2) Å] have similar values to those observed for other Mn–N (macrocycle) systems, and are shorter than those observed for Mn–O (macrocycle) equatorial bonds in the MnN_3O_2 complex.[21]

X-Band ESR results at room temperature

The solid line in Fig. 3(*a*) shows the ESR X-band powder spectrum at 300 K of complex **1** when diluted magnetically to 9.52% (w/w) in a diamagnetic rhodium matrix. The spectrum shows five well defined lines from zero to 7500 G (G = 10^{-4} T), but not hyperfine structure. The g value of this quintuplet is 2.111. The linewidth increases with increasing magnetic field, from 350 G for the leftmost line to 620 G for the rightmost line. Powder ESR spectra of this type have been reported previously[9,25–27] for manganese(II) seven-co-ordinated complexes. Such spectra have been interpreted using the spin Hamiltonian treatment of Dowsing and Gibson,[16] Griscom and Griscom[17] and Bleaney and Ingram[28] and more recently Mabbs and Collison[19] and it is written in equation (1) where the first term is the Zeeman

$$H = \boldsymbol{gBS}\cdot H + \boldsymbol{D}[S_z^2 - (1/3)S(S+1)] + \boldsymbol{E}(S_x^2 - S_y^2) + \boldsymbol{A}\,\boldsymbol{S}\cdot\boldsymbol{I} \quad (1)$$

interaction and the second and third terms correspond to the crystal-field splitting and the nuclear hyperfine interaction, respectively. The last term will not be considered any further

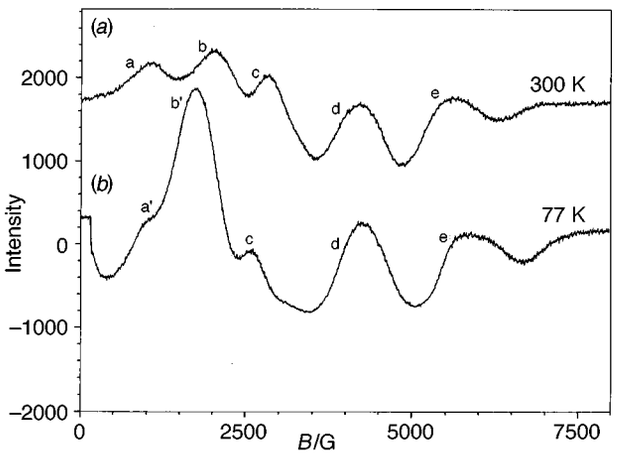

Fig. 3 X-Band powder ESR spectra of the $[MnL(H_2O)_2]Cl_2{\cdot}4H_2O$ complex obtained at (*a*) 300 K, microwave frequency 9.450 GHz, measured *g* value 2.111 and (*b*) 77 K, microwave frequency 9.0945 GHz. Sweep field 8000 G, modulation amplitude 0.5 G, gain 1000, time constant 0.03 s

since the complex did not show hyperfine splitting; ***D*** and ***E*** are the usual axial and rhombic crystal field parameters, respectively.[16–19,29] It is customary to define the parameter $\lambda = E/D$, which can take values between zero and 1/3, where the extreme value $\lambda = 0$ represents the totally axial case of the tensor ***D*** and the other extreme value $\lambda = 1/3$ represents the maximum rhombic distortion, $E = D/3$, of the crystal-field tensor. Values of λ outside this range reproduce the cases already included in the $0 < \lambda < 1/3$ range.[16–19,29]

Electron spin systems with $S > \frac{1}{2}$ for which λ and ***D*** are so small that they can be taken as zero give rise to ESR spectra centred around $g = 2$. Systems with large axial crystal fields with $\boldsymbol{D} \geqslant 0.25$ cm^{-1} and $\lambda = 0$ show an intense feature at $g = 6$ and a small feature at $g = 2$.[24,27,28] On the other hand, systems with large ***D*** and rhombicities with λ in the vicinity of 1/3 give rise to ESR spectra with sharp resonances at $g = 4.28$.[26–28] Complex **1** shows five fine-structure lines centred at $g = 2.111$, which are compatible only with total electron spin $S = \frac{5}{2}$ and parameters ***D*** and λ that are small, but not zero. The high-spin value deduced from ESR is consistent with that obtained from the room-temperature susceptibility measurements mentioned above. In consequence, the crystal electric field suggested is weak. In addition, the absence of resonances at $g = 6.0$ and 4.28 indicates also a weak crystal field with λ far from the extreme values zero and 1/3.

The measured *g* value of 2.111 is considerably far from 2.0, expected for $S = \frac{5}{2}$ systems experiencing very small crystal fields. Griscom and Griscom[17] have demonstrated that when ***D*** starts to be comparable to the Zeeman term, *i.e.* $(1/4)gBH$ or larger, the central fine transition $+\frac{1}{2} \leftrightarrow -\frac{1}{2}$ deviates from $g = 2.0$ towards higher *g* values and splits into two transitions, until it reaches the value of $g = 4.3$ for rhombic crystal fields, or even the value $g = 6.0$ for large axial crystal fields. The X-band spectrum of complex **1** in Fig. 3(*a*) clearly shows partial splitting and shifting towards *g* values higher than 2.0. Hence, for this compound, a first estimate of $\boldsymbol{D} \geqslant (1/4)gBH$, which implies that the crystal-field effects are not only not negligible, but are of the order of the Zeeman term, and a complete solution of equation (1) is required. On the other hand, the field positions of the five absorptions of the 300 K spectrum are consistent with the positions in the Dowsing and Gibson (DG) plots[16] for $0.055 \leqslant \boldsymbol{D} \leqslant 0.076$ cm^{-1} and $0.1 \leqslant \lambda \leqslant 0.15$. From these values *E* is estimated to be in the range 0.0055–0.0076 cm^{-1}. These first estimates of ***D*** and ***E*** were taken into account to solve the spin Hamiltonian (1) exactly, by matrix diagonalisation, since the perturbation theory cannot be applied. A computer program, using the MATLAB package, was written for this purpose.[15]

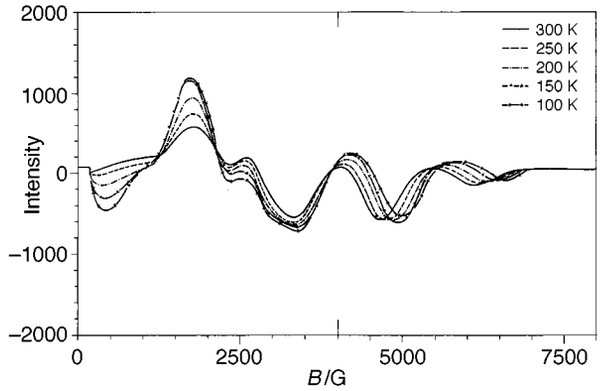

Fig. 4 Sequence of spectra taken every 50 K, from 300 to 100 K, of $[MnL(H_2O)_2]Cl_2{\cdot}4H_2O$

Exact numeric eigenfunctions, eigenenergies, transition probabilities and transition magnetic fields were calculated for the magnetic field *H*, parallel and perpendicular to each of the principal *X*, *Y* and *Z* axes. The line spectrum so calculated agreed completely with the experimental one, following standard procedures.[17,19] The deduced spin Hamiltonian parameters are $D = 0.07$ cm^{-1}, $E = 0.008$ cm^{-1} and $\lambda = 0.1142$. Hence, the crystal electric field is axial with a rhombic contribution, consistent with the distorted pentagonal-bipyrimidal geometry determined from the X-ray analysis.

The absence of the expected hyperfine structure from the manganese nuclear spin $I = \frac{5}{2}$ in the spectrum indicates that the magnetic dilution of 9.52% (w/w) in the rhodium matrix still represents a high concentration and dipole–dipole interactions prevent resolution of the hyperfine structure.[30] In addition, Birdy and Goodgame[31] and Wagnon and Jackels[27] have interpreted the lack of hyperfine splitting as a consequence of a relatively large amount of zero-field splitting, due to the crystal field, as is indeed the case for compound **1**.

It is quite interesting that this seven-co-ordinated manganese(II) complex, being an odd-electron Kramer system, shows all its five fine structure transitions well resolved, and the outer transitions have not spread out substantially. It is well known that for Kramer ions, such as Mn^{II}, a substantial broadening of the outer fine-structure transitions results from distribution in ***D*** and ***E*** and other spin Hamiltonian parameters, due to internal microscopic strains which are intrinsic to the samples.[17,18,30] Such effects do not influence the $+\frac{1}{2} \leftrightarrow -\frac{1}{2}$ transition of Kramer systems. In this case it seems that the molecular arrangement of **1** is so regular that the distribution of ***D*** and ***E***, in contrast to many other systems, is very sharp. In this sense the regularity allowed the definition of the ESR fine-structure lines and the X-ray determination with high precision.

X-Band ESR results at low temperature

The X-band ESR spectrum of complex **1** at 77 K is shown in Fig. 3(*b*). Several changes are quite clear: a large, negative and broad (500 G) spectral feature a′ appears at practically zero magnetic field. Also a very intense peak b′ has grown with its maximum at the apparent position $g = 3.66$. These changes prompted us to determine how the low-temperature features developed. Therefore, spectra were taken at several intermediate temperatures, and a set of these is presented in Fig. 4. The gradual growth of a′ and b′ [Fig. 3(*b*)] is clearly seen to start at a temperature of only 278 K. In addition, the rightmost lines opened up gradually with the temperature decrease to 100 K, and the position of the rightmost line shifted from 6005 to 6350 G, with concomitant increase in the axial parameter ***D*** of ≈58 G, its value being ≈0.0056 cm^{-1}. A temperature dependence of the axial crystal-field parameter ***D*** has been observed for several other manganese(II) systems.[32]

Since the low-temperature a′ and b′ features overlap greatly

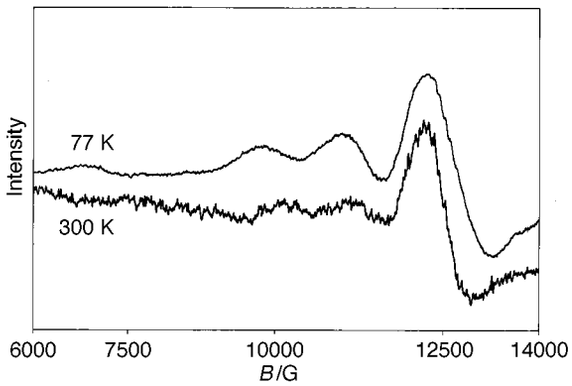

Fig. 5 Q-Band powder ESR spectra of the $[MnL(H_2O)_2]Cl_2 \cdot 4H_2O$ complex obtained at 300 K, microwave frequency 35.01 GHz, measured g value 2.00, and 77 K, microwave frequency 34.99 GHz. Sweep field 14 000 G, modulation amplitude 1.2 G, gain 3200, time constant 0.03 s

with three out of the five 300 K lines their line shapes are masked; however, the g value of 3.66, *i.e.* the maximum of peak b′, can be taken as representative. The b′ absorption, along with the close to zero-field absorption a′, clearly seen at low temperatures, and the DG plots,[16] allow us to estimate $\boldsymbol{D}$ as 0.074 cm^{-1} and $\boldsymbol{E}$ close to (1/3)$\boldsymbol{D}$. These parameters were used to calculate a low-temperature line spectrum, which is consistent with all the experimental features.

All these gradual, neat changes in temperature (Fig. 4) indicate a transformation, different from a phase transition, since for the latter to occur abrupt changes are expected.[33] Instead we propose a slight magnetostructural dependence on temperature for complex **1**, for which the behaviour of $\boldsymbol{D}$ and $\boldsymbol{E}$ with temperature, in turn, indicates that the crystal field becomes larger and with a higher rhombicity as the temperature decreases. The increase of the intensities of the a′ and b′ features with decreasing temperature is well accounted for by the Boltzmann population factor for paramagnetic systems.[18,30]

In order to examine whether the diamagnetic rhodium matrix has any effect on the magnetic behaviour described above, ESR spectra of frozen solutions (77 K) of complex **1** in dimethyl sulfoxide were obtained at X-band frequency. These spectra were practically identical to those obtained for the diamagnetic rhodium matrix dilutions of **1**, *i.e.* the magnetic changes with temperature already described are indeed intrinsic to the manganese compound.

Q-Band ESR results at room and low temperature

In order to confirm the evaluation of the spin Hamiltonian parameters, the Q-band spectra of complex **1**, at both 300 and 77 K, were recorded (Fig. 5). Three important transitions appear at 10 800, 12 450 and 13 850 G. it is presumed that the other two fine-structure lines could appear at ≈14 650 and ≈15 340 G, beyond the reach of our spectrometer. The band at 12 450 G is assigned to the central $+\frac{1}{2} \leftrightarrow -\frac{1}{2}$ transition, with $g = 2.0$. Theoretical Q-band line ESR spectra were calculated by using the X-band calculated parameters, and all the lines were very well reproduced, hence confirming our evaluations. In this case, the microwave quantum $h\nu_Q$ value increases to 1.22 cm^{-1}, while $\boldsymbol{D}$ and $\boldsymbol{E}$ remain constant. Under this condition the crystal-field effects are about four times smaller than in X-band, approximating more to a perturbation of the Zeeman term. Neither a zero-field transition nor a strong transition around $g = 4.0$ can be expected; second-order effects of the crystal field on the g value are not expected either, and the five fine-structure transition lines should be centred very close to $g = 2.0$. All these features are present in the 300 and 77 K Q-band ESR spectra in Fig. 5. At Q-band there is no variation of the spectrum with temperature, confirming that the X-band temperature changes are due to crystal-field variations.

Conclusion

We conclude that the ESR spectra indicate that at room temperature the crystal field is mainly rhombic, with $\lambda = 0.1142$, a result that is consistent with the distorted pentagonal-bipyramidal co-ordination geometry, determined from our X-ray experiments. As the temperature decreases $\boldsymbol{D}$ increases slightly and a larger rhombicity appears, with $\lambda = 0.162$ at 77 K. The Q-band results are fully consistent with the X-band determination. It is considered that the smooth crystal-field dependence on temperature is most likely related to small structural changes with temperature. Further, that if this is the case then a small torsion of the bonding angles of the axially co-ordinated water molecules in compound **1** is more likely to produce a slightly distorted crystal field than a distortion involving the pentagonal-base nitrogen bonds, for these seem to be more rigid and it would require more energy to distort them. The shifting of the 400 nm UV/VIS peak in solution to 445 nm in the solid state suggests that the electronic energy levels originating the transition have become closer, which is consistent with a geometrical change around the manganese(II) ion when passing from solution to the solid state. Therefore, the electronic structure of **1** seems to be very sensitive to the surroundings.

Acknowledgements

The authors are grateful to E. Basurto for his help with the software used in this work. M. E. S. T. and O. J. S. are grateful for the economical support to the DGAPA-UNAM research project IN213794. We would also like to thank Mrs. C. Vázquez for the thermogravimetric analysis. D. R. R. and R. Z. U. are grateful to CONACYT for the acquisition of the ESR spectrometer. M. J. R. is grateful to CONACYT for the acquisition of an X-ray diffractometer.

References

1 D. R. Williams, *The Metals of Life*, Van Nostrand-Reinhold, London, 1971; I. Bertini, H. B. Gray, S. J. Lippard and J. S. Valentine, *Bioinorganic Chemistry*, University Science Books, Lill Valey, CA, 1994.
2 G. W. Brudvig and R. H. Crabtree, *Proc. Natl. Acad. Sci. USA*, 1986, **83**, 4586.
3 D. L. Kepert, *Prog. Inorg. Chem.*, 1979, **25**, 41; M. G. B. Drew, A. H. bin Othman, W. E. Hill, P. McIlroy and S. M. Nelson, *Inorg. Chim. Acta*, 1975, **12**, L25; M. G. B. Drew, J. De O. Cabral, M. F. Cabral, F. S. Esho and S. M. Nelson, *J. Chem. Soc., Chem. Commun.*, 1979, 1033; M. M. Bishop, J. Lewis, T. D. O'Donoghue, P. R. Raithby and J. N. Ramsden, *J. Chem. Soc., Dalton Trans.*, 1980, 1390.
4 L. F. Lindoy, *The Chemistry of Macrocyclic Ligand Complexes*, Cambridge University Press, Cambridge, 1989, p. 9.
5 S. M. Nelson, *Pure Appl. Chem.*, 1980, **52**, 2461.
6 S. M. Nelson and D. H. Busch, *Inorg. Chem.*, 1969, **8**, 1859; E. Fleischer and S. Hawkinson, *J. Am. Chem. Soc.*, 1967, **89**, 720; M. G. B. Drew and S. M. Nelson, *Acta Crystallogr., Sect. A*, 1975, **31**, S140; D. H. Cook, D. E. Fenton, M. G. B. Drew, A. Rodgers, M. McCann and S. M. Nelson, *J. Chem. Soc., Dalton Trans.*, 1979, 414; M. G. B. Drew, A. H. bin Othman, S. G. McFall and S. M. Nelson, *J. Chem. Soc., Chem. Commun.*, 1975, 818; M. G. B. Drew, J. Grimshaw, P. D. A. McIlroy and S. M. Nelson, *J. Chem. Soc., Dalton Trans.*, 1976, 1388; M. G. B. Drew, A. H. bin Othman, P. D. A. McIlroy and S. M. Nelson, *Acta Crystallogr., Sect. B*, 1976, **32**, 1029; M. G. B. Drew, A. H. bin Othman and S. M. Nelson, *J. Chem. Soc., Dalton Trans.*, 1976, 1394.
7 F. Begun, M. S. Khan, S. Z. Haider, K. M. A. Malik, F. K. Khan and M. B. Hursthouse, *J. Bangladesh Acad. Sci.*, 1991, **15**, 185.
8 Y. Nishida, N. Tanaka, A. Yamazaki, T. Tokii, N. Hashimoto, K. Ide and K. Iwasawa, *Inorg. Chem.*, 1995, **34**, 3616.
9 A. Van Heuvelen, M. D. Lundeen, H. G. Hamilton, jun. and M. D. Alexander, *J. Chem. Phys.*, 1969, **50**, 489.
10 M. M. Humanes, Ph.D. Dissertation, University of Lisbon, 1984.
11 K. Nakanishi, *Infrared Absorption Spectroscopy*, Holden-Day, San Francisco, 2nd edn., 1977, pp. 42–51; K. Nakamoto, *Infrared and Raman Spectra of Inorganic and Coordination Compounds*, Wiley, New York, 4th edn., 1986, pp. 227–229.
12 N. Walker and D. Stuart, *Acta Crystallogr., Sect. A*, 1983, **39**, 158.

13 *International Tables for X-Ray Crystallography*, Kynoch Press, Birmingham, 1974, vol. 4.
14 D. J. Watkin, C. K. Prout, R. J. Carruthers, R. J. Betteridge and P. Betteridge, CRYSTALS, Issue 10, Chemical Crystallography Laboratory, Oxford, 1996.
15 E. Basurto-Uribe, *Simulación de Espectros EPR de Compuestos Lantánidos*, Master Degree Thesis, ESFM-IPN, México, 1996.
16 R. D. Dowsing and J. F. Gibson, *J. Chem. Phys.*, 1969, **50**, 294.
17 D. L. Griscom and R. E. Griscom, *J. Chem. Phys.*, 1967, **47**, 2711.
18 J. R. Pilbrow, *Transition Ion Electron Paramagnetic Resonance*, Clarendon Press, Oxford, 1990.
19 F. E. Mabbs and D. Collison, *Electron Paramagnetic Resonance of d Transition Metal Compounds*, Elsevier, Amsterdam, 1992.
20 M. D. Alexander, A. Van Heuvelen and H. G. Hamilton jun., *Inorg. Nucl. Chem. Lett.*, 1970, **6**, 445.
21 M. G. B. Drew, A. H. bin Othman, S. G. McFall, P. D. A. McIlroy and S. M. Nelson, *J. Chem. Soc.*, *Dalton Trans.*, 1977, 438.
22 A. B. P. Lever, *Inorganic Electronic Spectroscopy*, Elsevier, Amsterdam, 2nd end., 1984, p. 446.
23 M. G. B. Drew, A. H. bin Othman, S. G. McFall, P. D. A. McIlroy and S. M. Nelson, *J. Chem. Soc.*, *Dalton Trans.*, 1977, 1173.
24 M. G. B. Drew, A. H. bin Othamn and S. M. Nelson, *J. Chem. Soc.*, *Dalton Trans.*, 1994, 1394.
25 R. D. Dowsing, J. F. Gibson, D. M. L. Goodgame, D. Goodgame and P. J. Hayward, *J. Chem. Soc. A*, 1969, 1242.
26 J. E. Newton and S. C. Jackels, *J. Coord. Chem.*, 1988, **19**, 265.
27 B. K. Wagnon and S. C. Jackels, *Inorg. Chem.*, 1989, **28**, 1923.
28 B. Bleaney and D. J. E. Ingram, *Proc. R. Soc.*, *London*, *Ser. A*, 1951, **205**, 336.
29 R. D. Dowsing, J. F. Gibson, M. Goodgame and P. J. Haygood, *J. Chem. Soc. A*, 1970, 1133.
30 A. Abragam and B. Bleaney, *Electron Paramagnetic Resonance of Transition Ions*, Clarendon, Oxford, 1970.
31 R. B. Birdy and M. Goodgame, *Inorg. Chem.*, 1979, **18**, 172.
32 K. L. Wan, S. L. Hutton and J. E. Drumheller, *J. Chem. Phys.*, 1987, **86**, 3801; J. E. Drumheller and R. S. Rubins, *J. Chem. Phys.*, 1986, **85**, 1699; C. Benelli, D. Gatechi, C. Zanchini, R. J. Doedens, M. H. Dickman and L. C. Porter, *Inorg. Chem.*, 1986, **25**, 3453.
33 A. B. Pippard, *Classical Thermodynamics*, Cambridge University Press, Cambridge, 1966.

Received 16*th February* 1998; *Paper* 8/01292J